*Science of Sintering*, **50** (2018) 111-121

doi: https://doi.org/10.2298/SOS1801111K

UDK 532.74; 685.34.036

# Influence of Synthesis Conditions on Morphological Features of the SBA-15 Containing Only Elongated and Rounded/Spherical Grains

**Maja Kokunešoski[1*)], Zvezdana Baščarević[2], Zlatko Rakočević[1], Aleksandra Šaponjić [1], Đorđe Šaponjić [1], Dragana Jordanov[1], Biljana Babić[1]**

[1]University of Belgrade, Vinča Institute of Nuclear Sciences, P.O. Box 522, 11000 Belgrade, Serbia

[2]University of Belgrade, Institute for Multidisciplinary Research, Kneza Višeslava 1, 11030 Belgrade, Serbia

***Abstract:***

*Mesoporous silica SBA-15 materials of high specific surface area (~700 $m^2$ $g^{-1}$) were synthesized by using block copolymer Pluronic P123 as template and tetraethoxysilane as silica source. The obtained materials were characterized by XRD, nitrogen adsorption - desorption measurements, SEM, EDS and AFM analysis. It was found that small modifications of synthesis conditions influenced the morphological features of the synthesized SBA-15 samples. The SEM analysis had shown that the SBA-15 synthesized at lower temperature and longer time of reaction (80 °C, 48 h) provided elongated rod-shaped grains about 1μm long. The other sample synthesized at higher temperature and shorter time of reaction (100 °C, 24 h) had rounded grains and grains of regular spherical shape with diameters ranging from 0.5 to 2 μm. The EDS analysis confirmed that the particles of both synthesized samples were of the $SiO_2$ content. In addition, the AFM analysis had shown different surface morphologies of the materials synthesized under various conditions.*

***Keywords:*** *Mesoporous material; SBA-15; Synthesis conditions; Nanostructures; Spherical grains.*

## 1. Introduction

Since the mesoporous siliceous materials were synthesized [1-5], there has been an increasing interest in tailoring of these materials for potential applications in separation and adsorption processes, catalysis, etc. One of the most studied mesoporous siliceous materials is the SBA-15 (Santa Barbara No. 15). The SBA-15 can be synthesized in acidic environment from tetraethyl orthosilicate in the presence of amphiphilic poly (alkylene oxide)-type triblock copolymer, trade name Pluronic P123 [6, 7]. This amorphous material has large BET surface area with large pore diameter and thick pore walls [4].

Morphology is one of the main factors influencing the practical applications of the SBA-15 as a mesoporous material. The SBA-15 materials have attracted much attention due to their wide potential applications in the areas of catalysis, separation, adsorption, sensors, drug delivery, and nanotechnology. Different morphologies of the SBA-15, such as: fibers,

*) **Corresponding author:** majako@vinca.rs

platelets, spheres, monoliths, films, etc. can be synthesized by varying the reaction conditions during synthesis [8-12]. For example, spheres with diameters in the range of micrometer are of particular interest in separation processes [13-15]. The rodlike morphology of the SBA-15 is of interest due to its small dimensions, and thereby the possibility of fast adsorption and mass transfer. This has been proven useful in applications such as immobilization of enzymes [16-18] or as a template for mesoporous carbon [19].

Synthesis of the SBA-15 with spherical particles has already been described in the literature [11, 20-22] as well as the synthesis of the SBA-15 with rounded particles [23] that were used as template for synthesis of carbon copies with spherical particles.

The aim of this study was to investigate how minor changes in synthesis conditions like heating, stirring during synthesis, duration of the synthesis, aging, and heating during aging, influenced morphology of the SBA-15. In order to estimate the influence of parameters of synthesis on the structure of materials, we analyzed the SBA-15 materials, synthesized in different reaction solutions [24, 25]. Material SBA-15 aged at 80 °C has elongated rod-shaped grains the surface morphology of which is in line with the literature data [4]. The other SBA-15, aged at 100 °C, synthesized under the conditions according to the patent [26], has elongated grains and grains of regular spherical shapes.

The following methods are used for characterization of surfaces of the analyzed SBA-15 samples: X-ray diffraction, nitrogen adsorption-desorption measurements, scanning electron microscopy, energy dispersive X-ray analysis, and atomic force microscopy the imaging of which reveals the actual surface condition and gives precise data on the surface characteristics of the SBA-15 material.

The material made of different mesoporous materials, like the SBA-15, opens the possibility of obtaining materials of specific, for example catalytic behavior, which will be the subject of our future research.

## 2. Experimental

### 2.1. Synthesis of the SBA-15 samples

The SBA-15 samples are synthesized according to standard procedures [4], by using Pluronic P123 (non-ionic triblock copolymer, $EO_{20}PO_{70}O_{20}$, BASF) as a surfactant and tetraethoxysilane (TEOS, 98%) as a source of silica. A 4.0 g sample of Pluronic P123 is dissolved in 30 ml of distilled water and 120 g of 2M HCl solution and stirred at 35 °C for 1.5 h. 8.5 g of TEOS was added dropwise into the solution and vigorously stirred at the same temperature for 1.5 h. This was followed by prolonged stirring and subsequent aging. Bearing in mind that the structure and surface properties of the SBA-15 samples depend on time and temperature of aging [4], we have varied these two parameters. According to the method proposed by Zhao et al. [4], the mixture (sample SBA-15/80) was aged in two steps. First it was aged at 35 °C for 20 h and then at 80 °C for 48 h. According to the patent [26], mixture (sample SBA-15/100) was stirred at 35 °C for 22 h and aged at 100 °C for 24 h. The final products obtained by both methods were filtered, washed with 600 ml of distilled water, and dried at room temperature. Calcination was carried out in flowing air by slowly increasing the temperature from room temperature to 500 °C for 8 h and keeping it at 500 °C for 6 h to decompose tribloc copolymer.

### 2.2. Characterization of the SBA-15 samples

X-ray diffraction (XRD) patterns were recorded by using the BRUKER D8 advance diffractometer equipped with focusing Ge-crystal, the primary transmission input monochromator (Johanson type) that generates Cu Kα radiation (λ = 0.1546 nm). The range of 2°- 60° 2θ was used in a continuous scan mode with a scanning step size of 0.05° at step

time: 8 s. Adsorption and desorption isotherms of $N_2$ were measured on the SBA-15 samples at −196 °C using the gravimetric McBain method [27]. The specific surface area, $S_{BET}$, pore size distribution, mesopore including external surface area, $S_{meso}$, and micropore volume, $V_{mic}$, of the samples were calculated by using the obtained isotherms. Pore size distribution was estimated by applying the BJH method to the desorption branch of the isotherms. Mesopore surface and micropore volume were estimated by using the high-resolution $\alpha_s$ plot method [28-30]. Micropore surface, $S_{mic}$, was calculated by subtracting $S_{meso}$ from $S_{BET}$. Microstructure analysis was performed by a scanning electron microscope (SEM, VEGA TS 5130 MM, Tescan). X-ray microanalysis (EDS) was carried out using the INCA PentaFET-x3, Oxford Instruments. Carbon conductive tape was used to place powder samples on the SEM sample holders. Prior to the analysis, all samples were Au-Pd coated. Topography of the area investigated silica samples was performed by using the atomic force microscopy (AFM) Veeco MultiMode Quadrex type IIIe in tapping mode under ambient conditions with Veeco RTESP cantilever. Measuring probe was pyramid shaped peak height of 15-20 μm. Scanning speed was established at a frequency of 2 Hz in order to obtain optimal image quality.

## 3. Results and discussion

### 3.1. XRD analysis

The XRD pattern of the SBA-15/80 and the SBA-15/100 is shown in Fig. 1. Both samples, the SBA-15/80 and the SBA-15/100 exhibit a single very broad peak at about 23°, which is the characteristic of amorphous silica. XRD pattern of the SBA-15/100 sample exhibits a very broad peak which is stronger in comparison to the sample SBA-15/80.

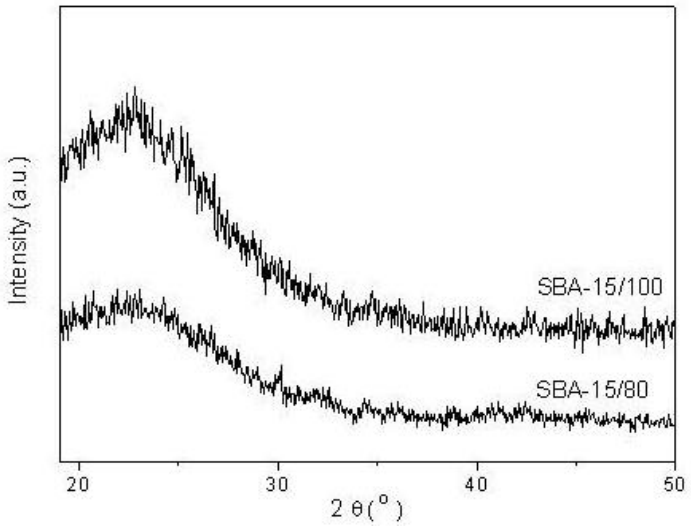


**Fig. 1.** XRD patterns of SBA-15/80 and SBA-15/100.

### 3.1. Adsorption isotherms - BET experiments

Nitrogen adsorption and desorption isotherms for samples of materials, i.e. the SBA-15/80 and the SBA-15/100 [24, 25], as a function of $N_2$ relative pressure and at −196 $^oC$ are displayed in Fig. 2. According to the IUPAC classification [31], the isotherms for both synthesized materials are of type-IV and with a hysteresis loop associated with mesoporous materials. The specific surface areas are calculated by the BET equation, $S_{BET}$. For the

samples SBA-15/80 and SBA-15/100, the $S_{BET}$ values are 710 $m^2$ $g^{-1}$ and 641 $m^2$ $g^{-1}$, respectively. Value of $S_{BET}$ decreases with increasing temperature of syntheses [24, 25]. It is obvious that the $S_{BET}$ value depends on the synthesis condition. Also, the $S_{BET}$ value of mesoporous materials decreases with increasing temperature of calcination [32].

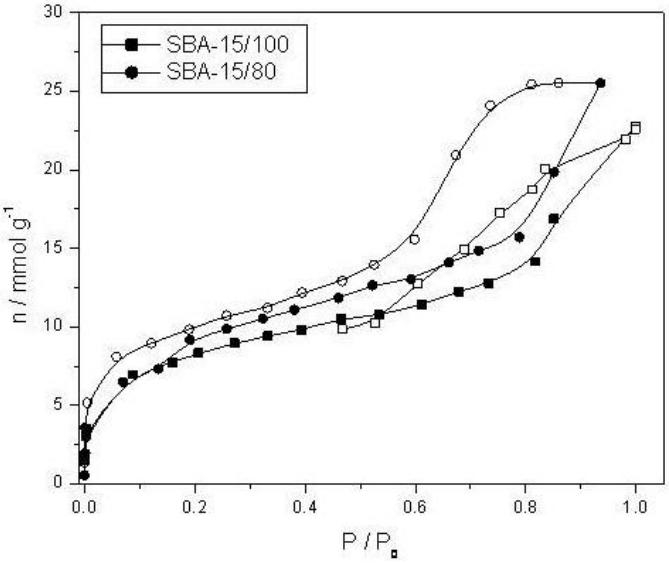


**Fig. 2.** Nitrogen adsorption and desorption isotherms, as a function of relative pressure for silica materials. Solid symbols - adsorption, open symbols - desorption.

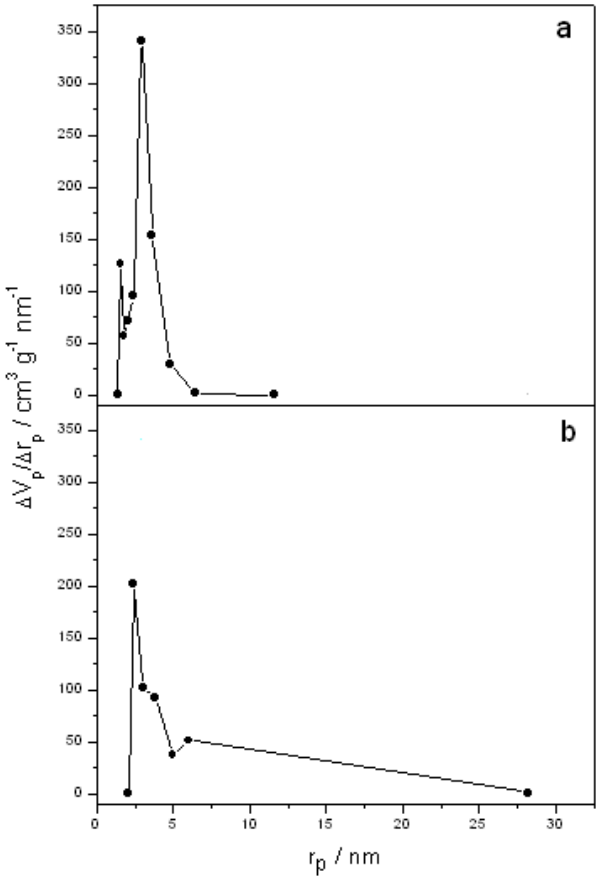


**Fig. 3.** PSD of (a) SBA-15/80 and (b) SBA-15/100.

The pore size distribution (PSD) of the samples, SBA-15/80 and SBA-15/100 [24, 25] is shown in Fig. 3. For the SBA-15/80, the pore radius (1.4 - 6 nm) has more narrow pore size distribution in comparison to the SBA-15/100 (1.9 - 25 nm). The PSD curves show that these samples are mesoporous.

### 3.3. SEM analysis

The SEM analyses of the SBA-15 synthesized siliceous materials are shown in Fig. 4. The material SBA-15/80 (Fig. 4(a, b)) consists of many elongated rod-shaped grains of relatively uniform sizes (up to 1μm). These elongated rod-shaped grains are laterally closely linked and aggregated into wheat-like structures. Similar chain agglomerate structures (Fig. 4(c)) were reported in an earlier paper [4]. The SBA-15/100 (Fig. 4(c, d)) has slightly rounded grains mostly smaller than 1 μm, which look like peanuts. These grains, due to their rounded form, have a small contact surface and smaller lateral connecting in relation to the elongated rod-shaped grains of the SBA-15/80 with large lateral contact area (Fig. 4(a)). The short chains of the SBA-15/100 agglomerates form a dense intertwined structure (Fig. 4(d)).

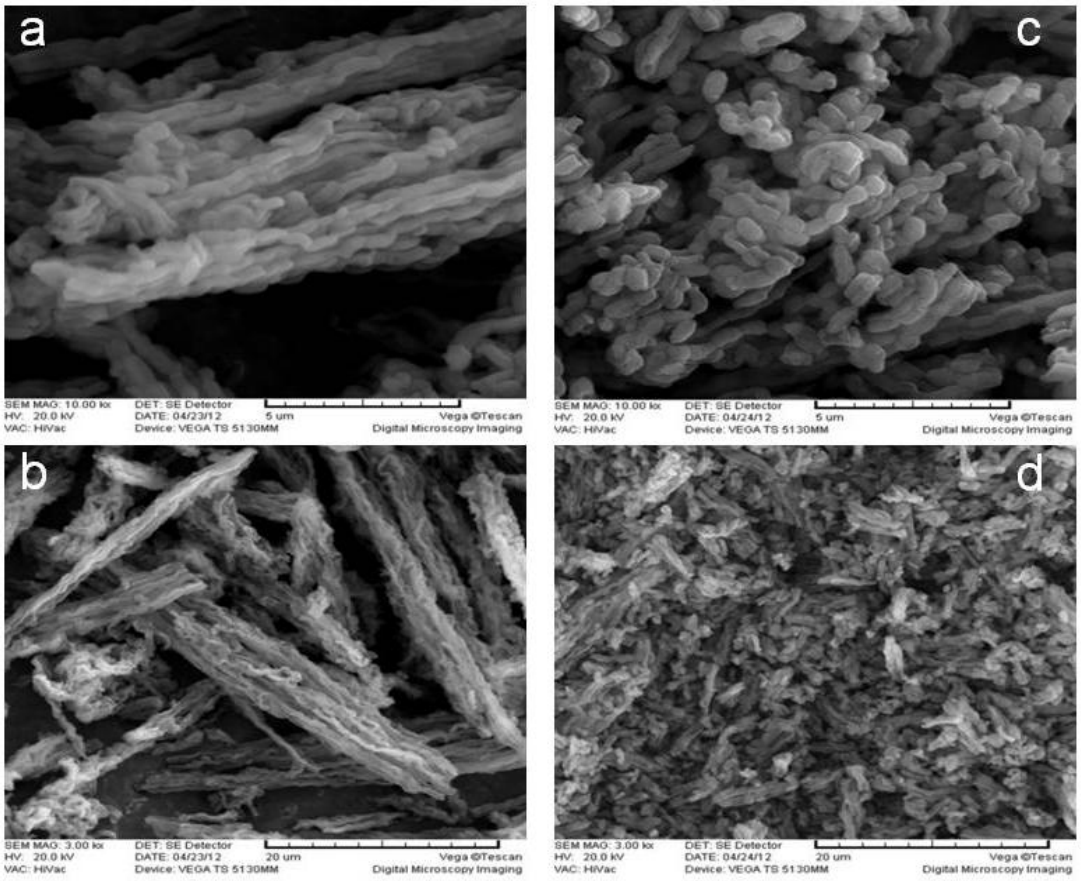


Fig. 4. SEM micrographs of (a, b) SBA-15/80 and (c, d) SBA-15/100.

Differences in grain shape and grain agglomerates between the SBA-15/80 and the SBA-15/100 are caused by different conditions of their synthesis. The grain form was influenced by stirring, aging time, and temperature at which the aging phase took place during the synthesis of these materials. Combination of the synthesis conditions, prolonged stirring at 35 $^{o}$C and aging at 100 $^{o}$C resulted in formation of a number of rounded grains (Fig. 4(c)). For the sample SBA-15/100, the combination of synthesis conditions leads to the formation of a

number of spheres which tend to build agglomerates (Figs. 5 and 6). The absence of stirring on the synthesis of monodisperse elongated grains connected to chains, as well as the influence of mixing on formation of round grains is reported in the literature [33]. In this material, the lateral weak connection between agglomerate chains has likely provided a free space in which spheres may be formed. The agglomerate of spherical particles with diameters ranging approximately from 0.5 to 2 μm, is presented in Fig. 5.

The form and size of the grains depend on the form and dimensions of the micelle which are formed from the surface active substance Pluronic P123 [34]. In addition to that, spherical and elongated grains are present, because Pluronic P123 has never formed only spheres due to very strong hydrophobic forces that lead to formation of elongated cylindrical silicate-surfactant micelles [35]. The micelles created by different conditions of synthesis were templates for forming of the grains in the SBA-15/80 and the SBA-15/100. The grains have obtained their final form by calcinations of these siliceous materials.

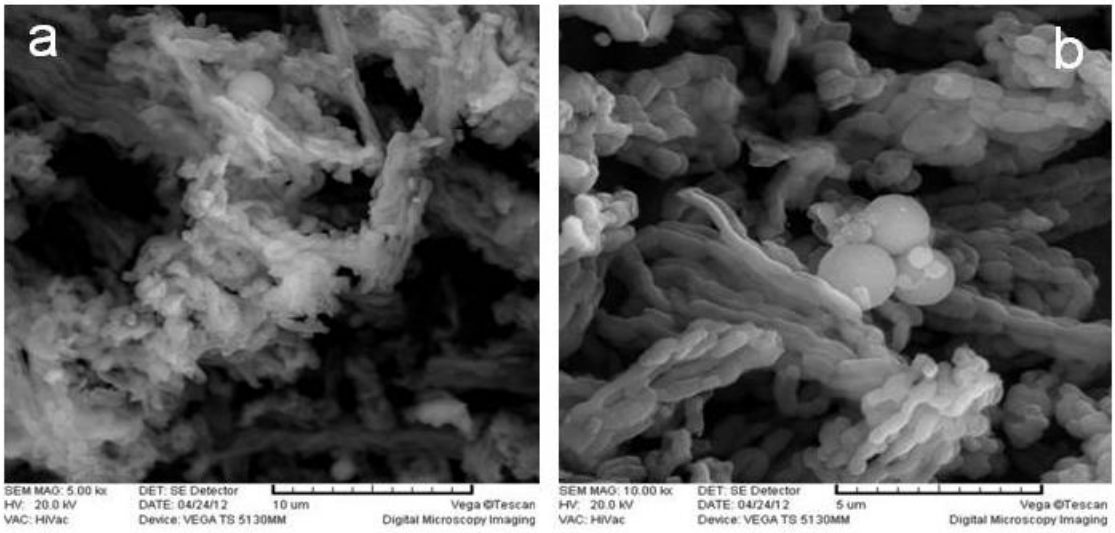


**Fig. 5.** SEM micrographs of the SBA-15/100.

## 3.4. EDS analysis

The EDS analysis of the SBA-15/100 surface content has demonstrated that the spherical particles in this sample are of $SiO_2$ content (Tab. I). Elemental analysis of the received SBA-15/80 and SBA-15/100 samples by using the Vario EL III; C, H, N, S/O Elemental Analyzer (Elemental, Germany) with thermal conductivity detector (TCD) showed that carbon was not present in the samples [25]. An experiment was performed at 1150 $^{o}$C in an He atmosphere. Amounts of the remained carbon in silica samples were below the detection limit of the instrument (0.3%). However, high levels of carbon (~ 30 at. %) and oxygen (~58 at. %) originate from gases from the air adsorbed by the surface of the samples (Tab. I). Successful application has already been reported of the SBA-15 in separation of carbon dioxide from mixtures with certain gases [36, 37]. Elements like palladium and gold originate from the Au-Pd coating applied prior to the analysis (Tab. I).

**Tab. I** EDS analysis of the SBA-15/100 sample (atomic %).

| Spectrum | C | O | Si | Pd | Au |
|---|---|---|---|---|---|
| ***Spectrum 1*** | 27.69 | 58.06 | 13.79 | 0.11 | 0.35 |
| ***Spectrum 2*** | 30.24 | 57.67 | 11.32 | 0.20 | 0.57 |

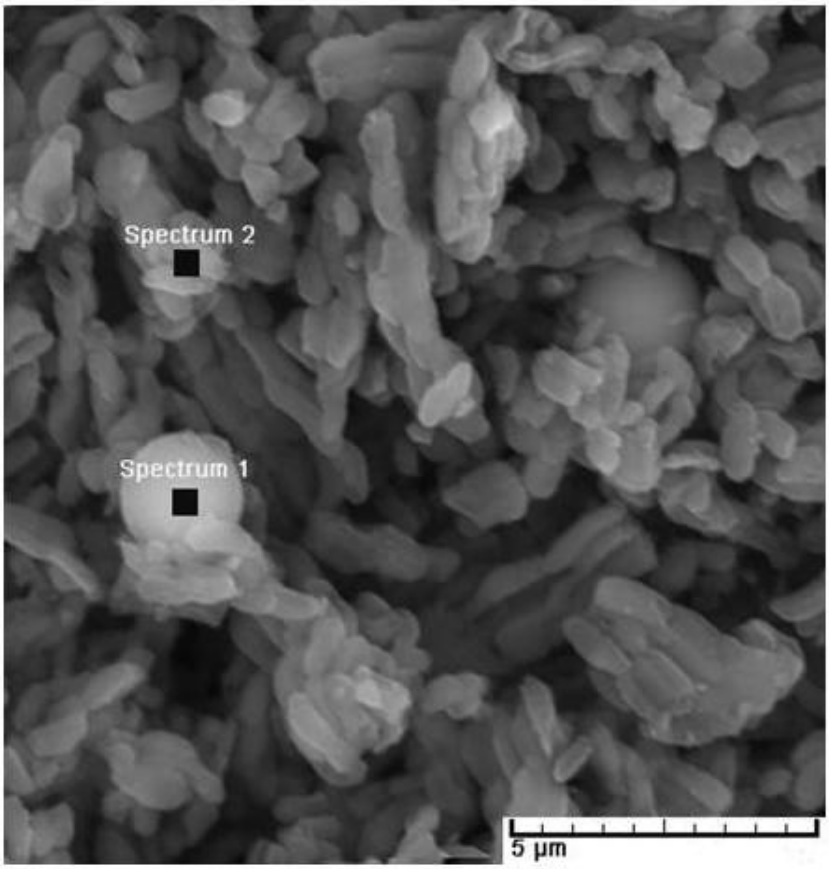


**Fig. 6.** SEM micrographs of the SBA-15/100 with the positions of EDS analysis (the positions correspond to the results presented in Tab. I).

## 3.5. AFM analysis

The AFM topological analysis has confirmed the influence of synthesis conditions on differences in the appearance and size of grains in the synthesized SBA-15 materials.

The AFM 3D-image of SBA-15/80 particle morphology is presented in Fig. 7(a). Material of the SBA-15/80 contains agglomerates about 75 nm long, which are made up of particles with the average size of approximately 6 nm. Sizes of the agglomerates and particles that form them have been estimated according to the horizontal distance of the positions between the cursors, used to mark the entities in the cross section of the observed agglomerate (Fig. 7(b)). In the same way we can estimate distances between particles of the agglomerate of about 6 nm which correspond to the size of pores obtained by PSD of the SBA-15/80 (Chapter 3.2). In the SBA-15/80 the aging phase was done without stirring at 35 $^{o}$C and then at 80 $^{o}$C. The synthesis conditions accomplished by stirring at 35 $^{o}$C and aging at 100 $^{o}$C resulted in the SBA-15/100 having a compact particle of about 150 nm (Fig. 8). That particle could be consistent with the particles of the peanut shape from the SEM micrograph of the same sample (Fig. 4(c)).

Hu and associates synthesized the SBA-15 at 95 $^{o}$C [38]. This procedure is similar to the procedure by means of which the SBA-15/100 is synthesized. By applying the AFM method, they determined the SBA-15 particle diameter to be at about 31 nm, which was smaller than the SBA-15/80 particle diameter (about 75 nm) and that of the SBA-15/100 (about 150 nm) which we had described in this study.

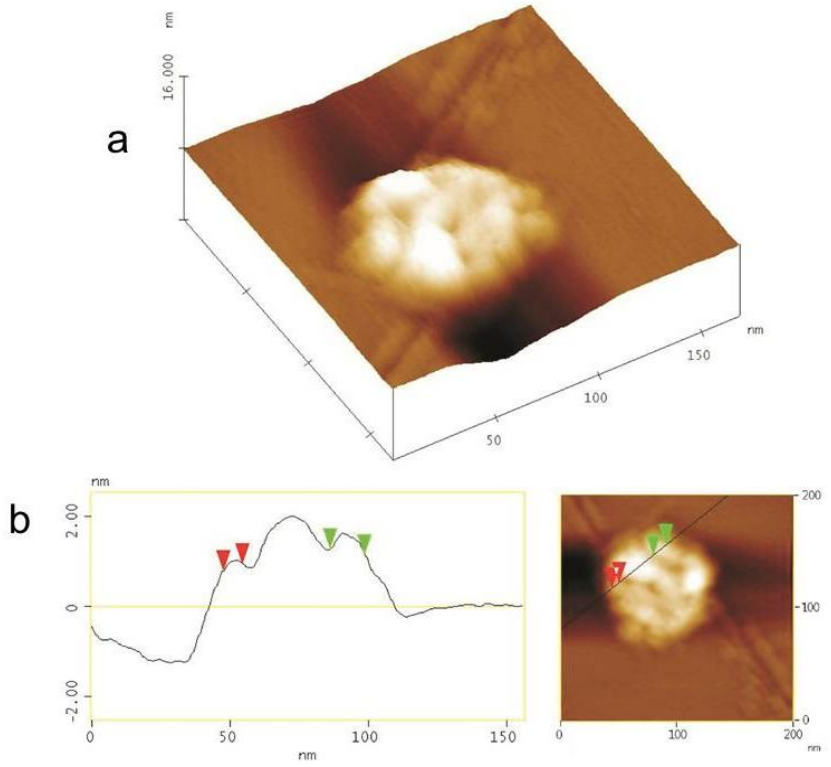


**Fig. 7.** AFM of SBA-15/80 particles: (a) appearance and (b) agglomerate cross section.

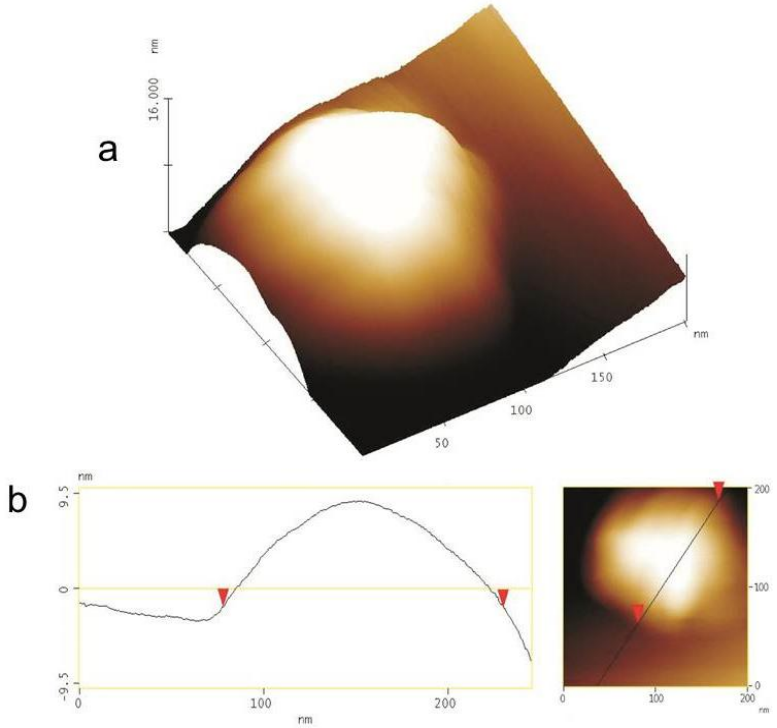


**Fig. 8.** AFM of SBA-15/100 particles: (a) appearance and (b) compact cross section.

After applying the SBA-15/80 i.e. SBA-15/100 onto the pyrolytic carbon surface (HOPG), this method demonstrated that these agglomerates differ in size and form. Small and light SBA-15/80 agglomerates have gathered along the HOPG surface terraces (Fig. 9(a)). The compact particles of the SBA-15/100 have distributed themselves evenly. These particles are almost the same in size and form (Fig. 9(b)). In Fig. 9(c) SBA-15/100 particles of almost uniform sizes i.e. about 130 nm are shown on the horizontal surface.

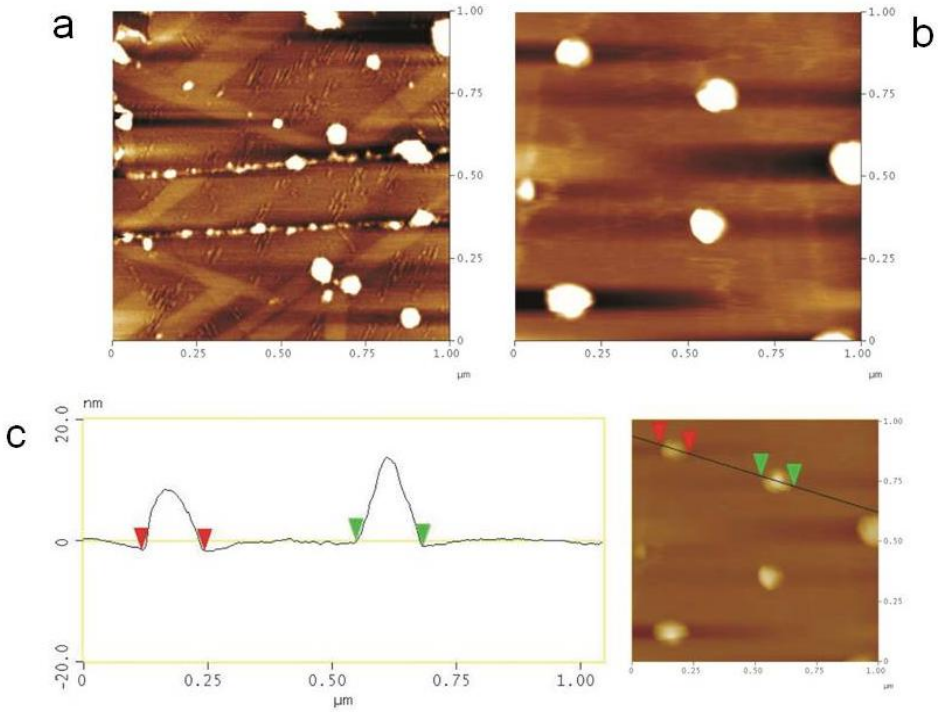


**Fig. 9.** AFM of particle on a base: (a) SBA-15/80, (b) SBA-15/100 as well as (c) cross section of the SBA-15/100 particle and base.

## 4. Conclusion

The differences in morphologies between the SBA-15 materials, which are synthesized by varying the synthesis conditions are featured in this study. The SEM and AFM topological analysis have confirmed that the synthesis conditions have made differences in size and form of the particles as well as in the morphology of the investigated materials. The grain form was influenced by stirring, aging time, and temperature at which the aging phase took place during the synthesis of these materials. The SBA-15, whose aging phase was at 80 $^{o}$C (lower temperature) and the prolonged reaction times (48 h) have elongated rod-shaped grain agglomerates about 1µm long. Other SBA-15 material, synthesized in the prolonged stirring conditions at 35 $^{o}$C, and then placed at 100 $^{o}$C (higher temperature) in a reaction which lasted a shorter period of time (24 h), have a few types of agglomerates consisting of the elongated, slightly rounded grains, and spherical particles. The elongated slightly rounded grains have an average length of up to 1 µm. Spherical particles with diameters of approximately 0.5 to 2 µm, also have a propensity for forming agglomerates. EDS analysis confirmed that all the present particles in this material are of $SiO_2$.

The insight into the morphogenesis of the SBA-15 provided by identifying the relationships between the morphological features and the synthesis conditions may also be useful for designing various nanostructured materials. The obtained mesoporous SBA-15

materials could be used as a carbon template for a variety of catalysts supports in fuel cell systems which will be the subject of our future research.

## Acknowledgements

This project was financially supported by the Ministry of Education, Science and Technological Development of the Republic of Serbia, in line with the contracts III-45012, III-45005 and OI-172045. The authors would also like to thank BASF Chemical Company for providing free samples of Pluronic P123. The authors are grateful to Vojislav Aranđelovic, Branislava Jovanovic and Miodrag Mitric for their help and support.

## 5. References

1. T. Yanagisawa, T. Shimizu, K. Kuroda, C. Kato, Bull. Chem. Soc. Jpn., 63 (1990) 988.
2. J. S. Beck, J. C. Vartuli, W. J. Roth, M. E. Leonowicz, C. T. Kresge, K. D. Schmitt, C. T.-W. Chu, D. H. Olson, E. W. Sheppard, S. B. McCullen, J. B. Higgins, J. L. Schlenkert, J. Am. Chem. Soc., 114 (1992) 10834.
3. B. G. Trewyn, I. I. Slowing, S. Giri, H. T. Chen, V. S.-Y. Lin, Acc. Chem. Res. 40 (2007) 846.
4. D. Zhao, J. Feng, Q. Huo, N. Melosh, G. H. Fredrickson, B. F. Chmelka, G. D. Stucky, Science, 279 (1998) 548.
5. D. Zhao, Q. Huo, J. Feng, B. F. Chmelka, G. D. Stucky, J. Am. Chem. Soc., 120 (1998) 6024.
6. P. Yang, D. Zhao, D. I. Margolese, B. F. Chmelka, G. D. Stucky, Nature 396 (1998) 152.
7. P. Yang, D. Zhao, D. I. Margolese, B. F. Chmelka, G. D. Stucky, Chem. Mater., 11 (1999) 2813.
8. Z. Jin, X. Wand, X. Cui, Z. Jin, X. Wand, X. Cui, Colloids Surf. A, 316 (2008) 27.
9. X. Y. Bao, X. S. Zhao, J. Phys. Chem. B, 109 (2005) 10727.
10. A. Sayari, B. Han, Y. Yang, J. Am. Chem. Soc., 126 (2004) 14348.
11. Proceedings: A. Carrero, J. Moreno, J. Aguado, G. Calleja in "4th International FEZA Conference" Eds. A. Gédéon, P. Massiani and F. Babonneau, Elsevier, Amsterdam, 2008, p. 321-24.
12. E. M. Johansson, M. A. Ballem, J. M. Cordoba, M-Oden, Langmuir, 27 (2011) 4994.
13. Y. R. Ma, L. M. Qi, J. M. Ma, Y. Q. Wu, O. Liu, H. M. Cheng, Colloids Surf. A, 229 (2003) 1.
14. H. H. Wan, L. Liu, C. M. Li, X. Y. Xue and X. M. Liang, J. Colloid Interface Sci., 337 (2009) 420.
15. H. I. Meléndez-Ortiz, B. Puente-Urbina, G. Castruita-de Leon, J. Manuel Mata-Padilla, L. García-Uriostegui, Ceramics International, 42 (2016) 7564.
16. J. Fan, J. Lei, L. Wang, C. Yu, B. Tu, D. Zhao, Chem. Commun., (2003) 2140.
17. J. Lei, J. Fan, C. Yu, L. Zhang, S. Jiang, B. Tu, D. Zhao, Micropor. Mesopor. Mat., 73 (2004) 121.
18. J. Sun, H. Zhang, R. Tian, M. Ding, X. Bao, D. S. Su, H. Zou, Chem. Commun., (2006) 1322.
19. C. Yu, J. Fan, B. Tian, D. Zhao, G. D. Stucky, Adv. Mater., 14 (2002) 1742.
20. A. Katiyar, S. Yadav, P. G. Smirniotis, N.G. Pinto, J. Chromatogr. A., 1122 (2006) 13.
21. X. Liu, L. Li, Y. Du, Z. Guo, T. T. Ong, Y. Chen, S. Choon Ng, Y. Yang, J. Chromatogr. A., 1216 (2009) 7767.
22. A. Szegedi, M. Popova, I. Goshev, J. Mihály, J. Solid State Chem., 184 (2011) 1201.

23. Y. Xia, R. Mokaya, Adv. Mater., 16 (2004) 1553.
24. M. Kokunešoski, J. Gulicovski, B. Matović, B. Babić, J. Optoelectron., 11 (2009) 1656.
25. M. Kokunešoski, J. Gulicovski, B. Matović, M. Logar, S.K. Milonjić, B. Babić, Mater. Chem. Phys., 124 (2010) 1248.
26. Patent, Block copolymer processing for mesostructured inorganic oxide materials, 6,592,764 July 15, 2003.
27. E. P. Barrett, L. G. Joyner, P. P. Halenda, J. Am. Chem. Soc., 73 (1951) 373.
28. K. Kaneko, C. Ishii, M. Ruike, H. Kuwabara, Carbon, 30 (1992) 1075.
29. M. Kruk, M. Jaroniec, K. P. Gadakaree, J. Colloid Interface Sci., 192 (1997) 250.
30. K. Kaneko, C. Ishii, H. Kanoh, Y. Hanzawa, N. Setoyama, T. Suzuki, Adv. Colloid Interface Sci., 76–77 (1998) 295.
31. K. S. W. Sing, D. H. Everett, R. A.W. Haul, L. Moscou, R. A. Pierotti, J. Rouquerol, T. Siemieniewska, Pure Appl. Chem., 57 (1985) 603.
32. A. Golubović, B. Simović, M. Šćepanović, D. Mijin, A. Matković, M. Grujić-Brojčin, B. Babić, Science of Sintering, 47 (2015) 41-49.
33. T. Benamor, L. Vidal, B. Lebeau, C. Marichal, Micropor. Mesopor. Mat., 153 (2012) 100.
34. V. L. Zholobenko, A. Y. Khodakov, M. Impéror-Clerc, D.Durand, I. Grillo, Adv. Colloid Interface Sci., 142 (2008) 67.
35. C. Yu, J. Fan, B. Tian, D. Zhao, Chem. Mater., 16 (2004) 889.
36. A. C. C. Chang, S. S. C. Chuang, M. Gray, Y. Soong, Energ Fuel, 17 (2003) 468.
37. Y. Sun, X.-W. Liu, W. Su, Y. Zhou, L. Zhou, Appl. Surf. Sci., 253 (2007) 5650.
38. X. Hu, X. Zhao, H. Hwang, Chemosphere, 66 (2007) 1618.

***Садржај:*** *Синтетисани су месопорозни силика материјали SBA-15, великих специфичних површина (~700 $m^2$ $g^{-1}$) применом блок кополимера комерцијалног назива Pluronic 123 template методом и применом тетраетхокисилане као изворoм силике. За карактеризацију материјала коришћене су следеће методе: рендгенска дифракциона анализа, метода адсдорпционо-десорпционих изотерма азота, скенирајућа електронска микроскопија, енергетски диспергована спектрометрија и микроскопија на основу атомске силе. Уочено је да су мале модификације услова синтезе утицале на морфолошке карактеристике синтетисаних SBA-15 узорака. Скенирајућа електронска микроскопија је показала да SBA-15 синтетан на нижој температури у дужем временском интервалу (80 °C, 48 h) има штапићаста зрна дуга до око 1 mm. Узорак синтетизује на вишој температури у краћем временском интервалу (100 °C, 24 h) има заобљене зрна и зрна сферног облика пречника у опсегу од 0.5 до 2 μm. Енергетски дисперговaном спектрометријом потврђено је да су честице оба синтетисана узорка изграђена од $SiO_2$. Микроскопија на основу атомске силе потврдила је разлике у морфологији површина материјала синтетисаних под различитим условима.*

***Кључне речи:*** *мезопорозни материјали; SBA-15; услови синтезе; наноструктуре; сферна зрна.*